Coordination of the Nuclear and Cytoplasmic Activities of p53 in Response to DNA Damage

Tian Pu, Xiao-Peng Zhang, Feng Liu,* and Wei Wang*
National Laboratory of Solid State Microstructures and Department of Physics, Nanjing University, Nanjing, China

ABSTRACT The tumor suppressor p53 plays a key role in the cellular response to various stresses. Most previous studies have focused on either the nuclear or cytoplasmic proapoptotic functions of p53, ignoring the combination of both functions. To explore how the two functions of p53 are coordinated in the DNA damage response via computer simulation, we construct a model for the p53 network comprising coupled positive and negative feedback loops involving p53, Mdm2, and Akt, as well as PUMA and Bax. In our model p53 is stabilized and accumulates in the nucleus and cytoplasm upon DNA damage. Nuclear p53 induces expression of *Mdm2, PTEN, PUMA*, and *Bax*. Cytoplasmic p53 is then released from the p53·Bcl-xL complex by PUMA to activate Bax directly. We find that the switching between low and high protein levels underlies the decision between cell survival and death. Moreover, a balance between the nuclear and cytoplasmic p53 levels and appropriate levels of Akt and PUMA are required for reliable cell fate decision. Our results indicate that coordination of the transcription-dependent and -independent activities of p53 is important in determining cellular outcomes. These findings advance our understanding of the mechanism for p53-mediated cellular responses and provide clues to p53-based cancer therapy.

INTRODUCTION

The tumor suppressor p53 is a central player in safeguarding the integrity of the genome. It plays a key role in the cellular response to various stresses including DNA damage, hypoxia, and oncogene activation (1,2). In unstressed cells, p53 levels are kept low by its negative regulator Mdm2 (3). Upon DNA damage, p53 can be stabilized and activated to induce cell cycle arrest, DNA repair, or apoptosis (2). Depending on the extent of DNA damage, cells either recover to normal proliferation or undergo apoptosis; that is, a decision between life and death is made by p53 signaling pathways (2).

p53 performs its function primarily as a nuclear transcription factor, regulating the expression of target genes to induce diverse cellular outcomes (4,5). For example, p53 can promote apoptosis through transactivating proapoptotic genes such as *PUMA* and *Bax*; such proapoptotic activity of p53 is crucial for suppressing tumorigenesis (6–8). On the other hand, apoptosis can be induced directly by the transcription-independent activity of p53 in the cytoplasm (9–11). Especially, p53 can activate Bax directly via transient protein-protein interactions (12).

Interestingly, the nuclear and cytoplasmic proapoptotic activities of p53 can be well coordinated by PUMA in response to genotoxic stress (13). Nuclear p53-inducible PUMA can displace cytoplasmic p53 from its inhibitor Bcl-xL so that p53 can activate Bax directly (12). Subsequently, mitochondrial outer membrane permeabilization (MOMP), the release of cytochrome *c*, and activation of caspase cascade can be induced to initiate apoptosis (14). Thus, the two seemingly separate activities of p53 can be combined into one single activity. Nevertheless, a couple of issues arise from the study of Chipuk et al. (13), including how the cell fate is determined by such coordinated p53 activities.

Moreover, cellular responses to DNA damage are also mediated by some prosurvival factors; among them, the serine-threonine kinase Akt is a major player (15). Akt promotes cell survival by suppressing the activities of proapoptotic proteins through phosphorylation (16). Thus, Akt and p53 regulate cellular outcomes in opposite ways. In fact, there exists a double-negative feedback loop among p53, Akt, and Mdm2 (17).

The p53 response to DNA damage may exhibit various modes, depending on cell and stress types (4). In an analog mode, a high (low) level of p53 leads to cell death (survival) in response to lethal (sublethal) DNA damage (2). By contrast, p53 levels can exhibit a series of discrete pulses in a digital mode (18). We and others have separately developed theoretical models to explore the mechanism for cell fate decision mediated by p53 pulses (19–21). Nevertheless, most previous studies center on either the nuclear or the cytoplasmic activity of p53, whereas coordination of the two functions of p53 is rarely investigated theoretically. Especially, the role of PUMA in the p53-mediated cellular response needs to be further clarified.

Motivated by the above considerations, here we develop a model for the p53 network in response to DNA damage, comprising the p53-Mdm2-Akt subnetwork as well as PUMA and Bax. Using numerical simulations, we correlate the temporal evolution of protein levels with the choice of cell fate. We demonstrate that the subcellular distribution of p53, the expression of PUMA and its affinity for Bcl-xL, and Akt levels remarkably affect the DNA damage response.

Submitted June 10, 2010, and accepted for publication July 22, 2010.

*Correspondence: fliu@nju.edu.cn or wangwei@nju.edu.cn

Editor: Andre Levchenko.

0006-3495/10/09/1696/10 $2.00

doi: 10.1016/j.bpj.2010.07.042

We highlight that coordination of the nuclear and cytoplasmic activities of p53 by PUMA subserves making optimal decisions. Our findings are consistent with experimental observations, and theoretical predictions are experimentally testable.

MODEL AND METHODS

This work is to clarify the mechanism for the response of HCT116 cells to ultraviolet (UV) radiation (13). The schematic diagram of the model is presented in Fig. 1. Our model for the p53-Mdm2-Akt subnetwork is an extension of Model Q3 in Wee and Aguda (22) by incorporating complex interactions and subcellular distribution of p53 and Mdm2. There exists a negative feedback loop between p53 and Mdm2, in which nuclear p53 induces expression of *Mdm2* and nuclear Mdm2 promotes degradation of p53 (3). This negative feedback is essential for maintaining low levels of p53 in unstressed cells. The presence of DNA damage enhances the degradation of nuclear Mdm2 and accumulation of p53. Moreover, there exists a positive feedback loop involving p53, Akt, and Mdm2. Nuclear p53 represses Akt activity indirectly, whereas Akt promotes the nuclear translocation of Mdm2 to degrade p53 (23). As a phosphatase, p53-inducible PTEN promotes the transition from PIP3 (Phosphatidylinositol 3,4,5-trisphosphate) to PIP2 (Phosphatidylinositol 4,5-biphosphate) (24,25). PIP3 is required for recruitment of Akt to the plasma membrane, where Akt becomes phosphorylated. As a kinase, Akt phosphorylates cytoplasmic Mdm2 and promotes its nuclear entry.

In our model, three forms of p53 are considered: $p53_n$ (nuclear p53), $p53_c$ (inactive form of cytoplasmic p53, i.e., p53 in complex with Bcl-xL), and $p53_c^*$ (active form of cytoplasmic p53, i.e., free p53). Three forms of Mdm2 are defined: $Mdm2_n$ (nuclear Mdm2), $Mdm2_c$ (dephosphorylated cytoplasmic Mdm2), and $Mdm2_{cp}$ (phosphorylated cytoplasmic Mdm2). Two forms of cytoplasmic Akt are distinguished between Akt (inactive, dephosphorylated form) and Akt_p (active, phosphorylated form). Note that activation of nuclear Akt can promote p53 stabilization in the response of lymphoblasts to ionizing radiation (26). However, no evidence supports the presence of this mechanism in HCT116 cells used by Chipuk et al. (13); thus, the effects of nuclear Akt are not considered in our model.

The activity of cytoplasmic p53 is initially sequestered by Bcl-xL (12). After DNA damage, p53 can be liberated from the p53·Bcl-xL complex by PUMA because it has a higher affinity for Bcl-xL than p53 does (13). In other words, it is PUMA that determines the status of cytoplasmic p53, whereas the total PUMA level ($[PUMA]_T$) is mainly controlled by nuclear p53. Here, PUMA molecules that are able to release cytoplasmic p53 are denoted by PUMA*, whereas those in complex with Bcl-xL are represented by $PUMA_{in}$.

Free cytoplasmic p53 can activate Bax directly to induce apoptosis (12). Here, we consider two forms of Bax: inactive Bax (Bax_{in}) whose activity is inhibited by the neutralization effects of Bcl-2, and active Bax (Bax*) that can oligomerize and form lipid pores on the mitochondrial membrane to induce MOMP (14). It is assumed that cytoplasmic p53 acts as an activator to promote the conversion from the inactive to active form of Bax. p53 does not form a stable complex with Bax; rather, they interact via the hit-and-run mechanism, and the activation of Bax results from a conformational change (27). The events after Bax activation are not characterized here. We simply consider persistent activation of Bax as a marker of apoptosis induction.

The dynamics of the model are characterized by ordinary differential equations, which are presented in the Appendix, and a set of standard parameter values is listed in Table 1. Note that oscillations in p53 levels

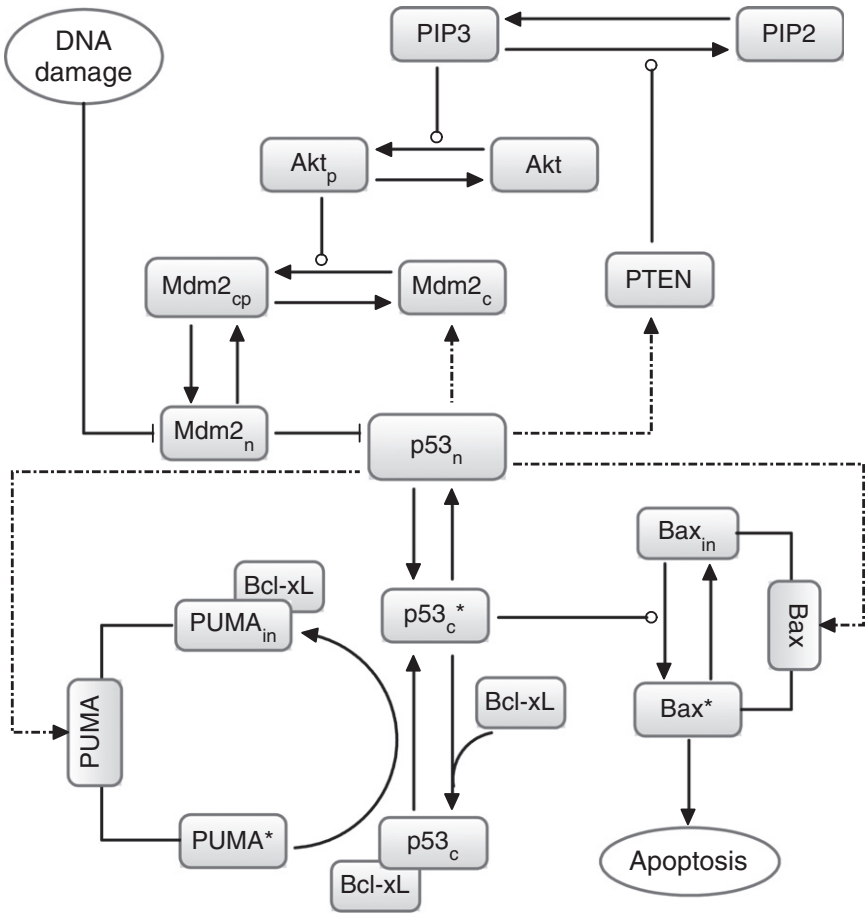

FIGURE 1 Schematic diagram of the model for the p53 network in response to DNA damage. There exists a negative feedback loop between p53 and Mdm2 and a double-negative one involving p53, Akt, and Mdm2. Both the nuclear and cytoplasmic forms of p53 and Mdm2 are considered, whereas only the cytoplasmic forms of other proteins are included. DNA damage enhances the degradation of nuclear Mdm2, and sustained activation of Bax induces apoptosis. (*Dot-dashed lines*) p53-induced gene expression. (*Arrowed lines*) Translocation of molecules or transitions between proteins (promotion of which is denoted by *circle-headed lines*).

TABLE 1 A set of standard parameter values

Parameter	Unit	Value	Parameter	Unit	Value
k_{rep}	min^{-1}	0.0055	k_{aktp}	min^{-1}	20
k_{p53n}	min^{-1}	0.8	J_{aktp}	μM	0.1
k_{p53c}	min^{-1}	2	k_{aktdp}	$\mu M/min$	0.2
k_{dmp53n}	min^{-1}	0.5	J_{aktdp}	μM	0.4
J_{dmp53n}	μM	0.01	k_{PIP3}	$\mu M/min$	0.5
k_{dp53n}	min^{-1}	0.04	J_{PIP3}	μM	0.2
k_{p53i}	$\mu M^{-1}min^{-1}$	0.3	k_{PIP2}	min^{-1}	22
k_{p53a}	$\mu M^{-1}min^{-1}$	3	J_{PIP2}	μM	0.01
k_{p53a0}	min^{-1}	0.01	k_{PTEN}	$\mu M/min$	0.001
k_{dp53bx}	min^{-1}	0.025	k'_{PTEN}	$\mu M/min$	0.07
k_{p53}	$\mu M/min$	0.1	J_2	μM	1.2
k_{dp53cs}	min^{-1}	0.01	k_{dPTEN}	min^{-1}	0.018
$k_{dmp53cs}$	min^{-1}	0.01	k_B	$\mu M/min$	0.2
$J_{dmp53cs}$	μM	0.15	k_{dB}	min^{-1}	0.1
k_{m2n}	min^{-1}	0.1	k_{puma}	$\mu M/min$	0.0002
k_{m2c}	min^{-1}	1	k'_{puma}	$\mu M/min$	0.16
k_{dm2n}	min^{-1}	0.01	J_3	μM	1.2
k_{dm2n0}	min^{-1}	0.04	k_{dpuma}	min^{-1}	0.05
k_{m2}	$\mu M/min$	0.018	k_{pumai}	$\mu M^{-1}min^{-1}$	0.2
k'_{m2}	$\mu M/min$	0.024	k_{pumaa0}	min^{-1}	0.1
J_1	μM	1.6	k_{bax}	$\mu M/min$	0.0001
k_{m2dp}	$\mu M/min$	0.2	k'_{bax}	$\mu M/min$	0.06
J_{m2dp}	μM	0.05	J_4	μM	1.2
k_{m2p}	min^{-1}	10	k_{dbax}	min^{-1}	0.01
J_{m2p}	μM	0.3	k_{baxa}	$\mu M^{-1}min^{-1}$	2
k_{dm2c}	min^{-1}	0.01	k_{baxi}	min^{-1}	0.5
k_{dm2cp}	min^{-1}	0.01			

were mainly observed in cellular responses to ionizing radiation (18). Because p53 levels exhibit switchlike behaviors in Chipuk et al. (13), we will not investigate the oscillatory dynamics of p53 in this work.

Considering the cooperativity of the tetrameric form of p53 as a transcription factor, the rate of p53-induced gene expression is typically characterized by a fourth-order Hill function of p53 level (20,28). To our knowledge, few models were constructed to describe the p53 response to UV radiation. With limited experimental data available, we still assume the Hill coefficient to be 4. Moreover, our simulation results indicate that the conclusions drawn here qualitatively hold true when changing the value of the coefficient. The Michaelis-Menten kinetics are used to characterize the reactions involving phosphorylation and dephosphorylation. Mdm2-targeted proteasomal degradation of p53 also obeys the Michaelis-Menten kinetics, whereas the basal degradation of proteins is modeled as first-order reactions.

It is noted that cyclobutane pyrimidine dimers (CPDs) are the main form of DNA damage induced by UVB (one kind of UV light as used by Chipuk et al. (13)), and on average 4.4 CPDs are produced per Mbp per J/m^2 UVB (29). Given the average length of human DNA (~6×10^9 bp), it is estimated that ~2.6×10^5 CPDs per cell can be produced at 10 J/m^2 UVB. We divide the initial number of CPDs produced at each dose of UVB by 2.6×10^5 and denote it by DNA^0_{dam}, which is used to characterize the initial extent of DNA damage. For the sake of simplicity, we assume that DNA damage is repaired at a constant rate and that the degradation rate of $Mdm2_n$ increases linearly with the extent of DNA damage.

Several other assumptions are made to simplify the model:

First, the total amount of Bcl-xL is assumed to be constant, because it was shown experimentally that Bcl-xL expression remains unchanged after UV treatment in HCT116 cells (13).

Second, the production and degradation of Akt are very slow, with its normal half-life being tens of hours, whereas the (de)phosphorylation of Akt is much faster. It was experimentally shown that even after radiation, Akt levels remain nearly unchanged (17). Thus, the total Akt level ($[Akt]_T$) is assumed to be constant.

Third, the total amount of PIP2 and PIP3, $[PIP]_T$, is also assumed to be constant.

Fourth, although cell cycle arrest is not explicitly modeled here, it is implicitly assumed to appear immediately upon DNA damage.

Integration of differential equations is performed using a fourth-order Runge-Kutta method with a time step of 0.01 min. On each simulation trial, the initial concentration of each species is set to its lower stable steady-state value. The values of $[Akt]_T$ and $[PIP]_T$ are set to 0.5 μM and 1 μM, respectively, unless specified otherwise.

RESULTS

p53-mediated cell fate decision

We first illustrate how the p53 network responds to different levels of DNA damage. Upon severe damage, $p53_n$ level first increases because of enhanced degradation of Mdm2 (Fig. 2 *A*). The levels of Mdm2, PTEN, PUMA, and Bax then rise as a result of nuclear p53-induced gene expression. PTEN inhibits the nuclear entry of Mdm2, resulting in a further increase in $p53_n$ level. Thus, the total levels of PUMA and Bax quickly rise in a switchlike manner. PUMA liberates cytoplasmic p53 from its interaction with Bcl-xL, leading to an increase in $p53^*_c$ level. Subsequently, $p53^*_c$ activates Bax, and the concentration of Bax* rises to a high level with a marked delay. Notably, the levels of these proteins are maintained around their maxima for a long time. According to the experimental observations that Bax induces MOMP and release of cytochrome *c* within 15 min after its activation (30,31), we assume that apoptosis will be initiated once Bax* level remains above some threshold (~2.1 μM, see below) for >30 min. Thus, the cell will undergo apoptosis in this case. By contrast, when DNA damage is slight or moderate, the amounts of those proteins rise gradually and then drop quickly to basal levels (Fig. 2 *B*). In this case, DNA damage can be fixed within a relatively short period and the cell survives. Thus, transient activation of Bax cannot induce apoptosis compared with its sustained activation.

It is noted that those proteins always return to their basal levels after DNA repair in our model. This is because we did

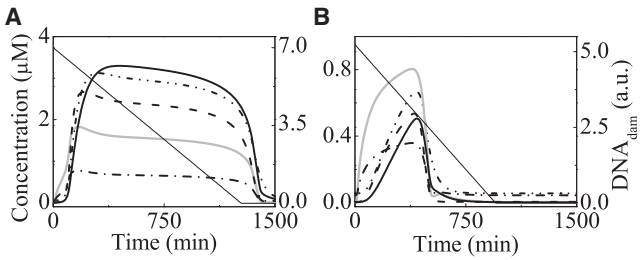

FIGURE 2 Temporal evolution of protein levels in response to DNA damage. The initial stress level is 7.0 (*A*) or 5.2 (*B*). Each panel shows time courses of the levels of $p53_n$ (*shaded line*), $p53^*_c$ (*dash-dotted line*), PTEN (*dash-dot-dotted line*), total PUMA (*dashed line*), and Bax* (*solid line*). The extent of DNA damage (*thin line*) decreases linearly because of the repair process. Depending on the initial stress level, the cell undergoes apoptosis (*A*) or survives after DNA damage is fixed (*B*).

not consider the effects of downstream apoptotic events on DNA repair-related proteins and p53. Actually, the activation of caspases after apoptosis initiation may cleave a number of proteins including the components of DNA repair machinery and p53 (32). We did not model these complicated effects, but only consider sustained activation of Bax as a marker of apoptosis induction.

We then systematically explore the dependence of cell fate on the initial stress level. The first step is to analyze the steady-state solution of the model as a function of DNA damage level, DNA_{dam}. $p53_n$ and Bax* levels exhibit bistability over the same range between 0.64 and 4.38 (Fig. 3). When moving rightwards across the upper threshold along the lower stable branch, $p53_n$ and Bax* levels jump to the higher stable state, and their values change slightly with further increasing DNA_{dam}. When moving leftwards across the lower threshold along the higher stable branch, $p53_n$ and Bax* levels drop to very small values from 1.22 and 2.11 μM, respectively. Such switchlike activation of Bax has previously been proposed (33). As will be seen later, the switching between the lower and higher states underlies the decision between cell life and death.

Actually, the extent of DNA damage decreases with the progression of DNA repair rather than being kept fixed. If Bax* level is larger than 2.1 μM only transiently, no apoptosis is induced. It is still necessary to determine cell fates based on the temporal evolution of protein levels. The simulation results for various stress levels are displayed in Fig. 4. The amounts of proteins can be maintained in the high-level state for a long period or be close to 0; accordingly, cells either die or live. Nuclear p53 levels are kept low in response to mild DNA damage (say $DNA^0_{dam} = 4.0$) (Fig. 4 *A*), and little Bax is activated (Fig. 4 *B*). Thus, the cell survives after DNA damage is repaired. With moderate DNA damage (e.g., $DNA^0_{dam} = 5.2$), both nuclear p53 and Bax are activated transiently, and such transient activation is insufficient to reach the threshold for apoptosis induction. At high stress levels (say $DNA^0_{dam} = 6.0$), both $p53_n$ and

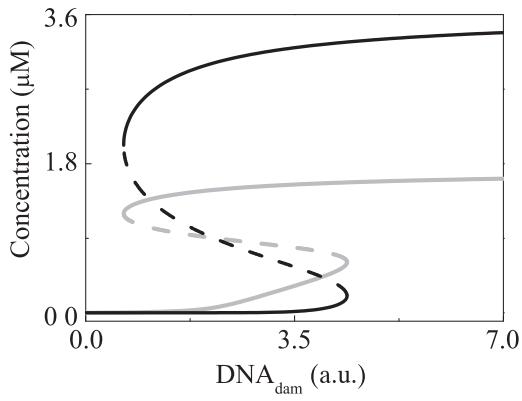

FIGURE 3 Steady-state bifurcation diagram of the levels of $p53_n$ (*shaded curve*) and Bax* (*black curve*) as a function of stress level, DNA_{dam}. (*Solid* and *dashed lines*) Stable and unstable states, respectively.

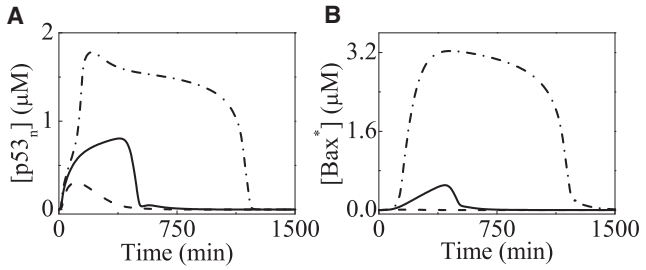

FIGURE 4 Temporal evolution of the levels of $p53_n$ (*A*) and Bax* (*B*) in response to DNA damage with $DNA^0_{dam} = 4.0$ (*dashed lines*), 5.2 (*solid lines*), or 6.0 (*dash-dotted lines*).

Bax* levels are kept around their maxima for a long time, and thus apoptosis is initiated. Therefore, the choice of cell fate is associated with the switching between low and high protein levels. With the standard parameter values used (see Table 1), cells survive when $DNA^0_{dam} < 5.3$ (i.e., the dose of UV is smaller than 53 J/m^2) or undergo apoptosis otherwise. This is consistent with the experimental observations (13).

Role of PUMA in cell fate decision

It has been experimentally shown that PUMA can couple the nuclear and cytoplasmic proapoptotic functions of p53 (13). Here, we systematically explore the role of PUMA in cell fate decision.

First, we investigate the importance of PUMA in apoptosis induction by changing the value of the maximal p53-inducible synthesis rate of PUMA, k'_{puma}. Note that the total Bax level is nearly independent of k'_{puma}. Differently, the total PUMA level depends remarkably on k'_{puma} (Fig. 5 *A*). For small k'_{puma} (say 0.068 μM/min), there is only weak expression of PUMA, while a small fraction of Bax is transiently activated (Fig. 5 *B*); no apoptosis is triggered. For moderate k'_{puma} (e.g., 0.15 μM/min), the amount of PUMA is sufficient to evoke significant activation of Bax, and apoptosis is initiated. For large k'_{puma} (say 0.3 μM/min), PUMA level rises remarkably while Bax* level varies slightly, compared with the case of $k'_{puma} = 0.15$. Therefore,

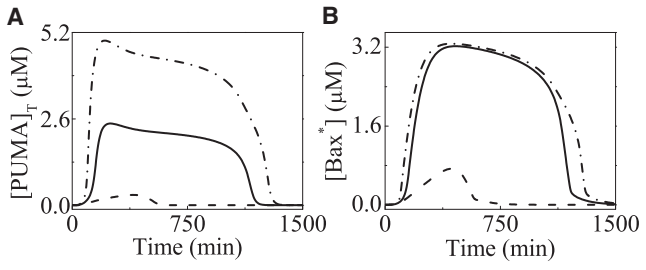

FIGURE 5 Effect of PUMA expression on apoptosis induction. Temporal evolution of $[PUMA]_T$ (*A*) and Bax* level (*B*) with $k'_{puma} = 0.068$ (*dashed lines*), 0.15 (*solid lines*), or 0.30 μM/min (*dash-dotted lines*). The initial DNA damage level is 6.0.

despite high-level expression of Bax, weak PUMA expression makes cells resistant to stress. Presumably, low levels of PUMA may result from low binding affinity of p53 to the promoter of *PUMA*. Actually, weak PUMA expression may be an important prognostic marker for some human cancers (34,35).

The activation of Bax requires that PUMA bind Bcl-xL to replace cytoplasmic p53 in addition to high-level expression of PUMA and Bax. To see this clearly, we systematically change the value of k_{p53a}, which characterizes the binding affinity of PUMA to Bcl-xL. When k_{p53a} is small (say 0.01 μM^{-1} min^{-1}), a small fraction of cytoplasmic p53 is released from Bcl-xL. Thus, only a small amount of Bax is transiently activated, and no apoptosis is initiated even in severely damaged cells (Fig. 6 *A*). When k_{p53a} is large enough, both cytoplasmic p53 and Bax are activated to induce apoptosis. On the other hand, for very large k_{p53a} (e.g., 15 μM^{-1} min^{-1}), a large fraction of cytoplasmic p53 is released from Bcl-xL, and Bax* level is high enough to initiate apoptosis even at moderate stress intensity (Fig. 6 *B*). Therefore, appropriate affinity of PUMA for Bcl-xL is crucial for optimal cell fate decision.

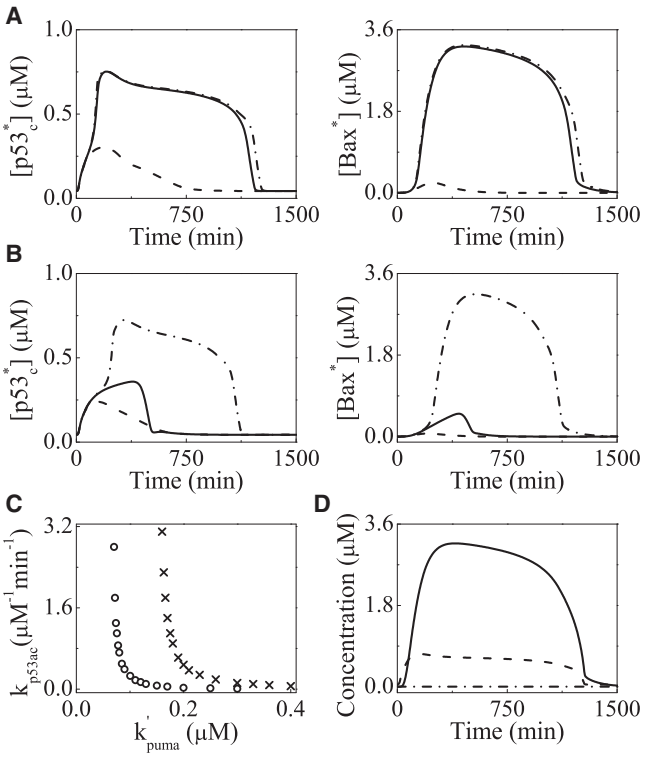

FIGURE 6 Effect of binding affinity of PUMA to Bcl-xL on cell fate decision. (*A* and *B*) The initial stress level is 6.0 (*A*) or 5.2 (*B*). Temporal evolution of the levels of $p53^*_c$ (*left column*) and Bax* (*right column*) with k_{p53a} = 0.01 (*dashed lines*), 3 (*solid lines*), or 15 μM^{-1} min^{-1} (*dash-dotted lines*). (*C*) For each given k'_{puma} and initial stress level, there exists a minimum of k_{p53a} for apoptosis induction, k_{p53ac}. The panel shows k_{p53ac} versus k'_{puma} with DNA^0_{dam} = 6.0 (*circle*) or 5.2 (*cross*). (*D*) Temporal evolution of $[PUMA]_T$ (*dash-dotted line*), $p53^*_c$ (*dashed line*), and Bax* (*solid line*) levels with k_{53i} = 0.003 μM^{-1} min^{-1}, k'_{puma} = 0, and DNA^0_{dam} = 6.0.

The results for the case of small k_{p53a} are consistent with the experimental observation by Chipuk et al. (13). They used mutant Bcl-xL that binds p53 rather than PUMA to make cells resistant to p53-induced apoptosis irrespective of PUMA expression. By analogy, we propose that mutation in PUMA may also impair its preferential binding to Bcl-xL, undermining its ability to release p53 from Bcl-xL. That is, the affinity of PUMA for Bcl-xL affects cellular sensitivity to apoptotic signals. A higher affinity makes cells more prone to die, whereas a lower affinity makes cells more resistant to DNA damage. It would be intriguing to test this experimentally.

The above results suggest that a tradeoff between cell life and death requires appropriate values of k_{p53a} and k'_{puma}. To make this point clear, we further investigate the combinatory effect of k_{p53a} and k'_{puma} on cellular outcomes. For a fixed initial stress level, we calculate the minimum of k_{p53a} for apoptosis induction at each k'_{puma} and denote it by k_{p53ac}. k_{p53ac} decreases with increasing k'_{puma} (Fig. 6 *C*). For a larger synthesis rate of PUMA, weaker binding affinity of PUMA to Bcl-xL is required to trigger apoptosis, and vice versa. That is, the p53-induced expression of PUMA and the release of p53 from Bcl-xL by PUMA complement each other in apoptosis induction. On the other hand, for small k'_{puma}, k_{p53ac} becomes much smaller in response to severe DNA damage compared with the response to mild DNA damage. Therefore, both the expression of PUMA and its affinity for Bcl-xL should be within a proper range so that cells can survive after repairable DNA damage is fixed or undergo apoptosis otherwise. Together, both the nuclear and cytoplasmic functions of p53 are significant in cell fate decision, and PUMA acts as an important coordinator.

The interaction between p53 and Bcl-xL may also be disrupted owing to some mutation in Bcl-xL or the presence of small-molecule inhibitors such as pifithrin-μ (PFT-μ). PFT-μ can remarkably reduce the binding affinity of p53 to Bcl-xL but has no effect on its transcriptional function (36). This implies that PFT-μ may promote accumulation of free cytoplasmic p53. We mimic this effect of PFT-μ by decreasing the inactivation rate of $p53^*_c$, k_{p53i}, from 0.3 to 0.003 μM^{-1} min^{-1} and setting k'_{puma} = 0. At high DNA damage levels, despite very low PUMA level, most cytoplasmic p53 molecules are free from the inhibition of Bcl-xL, resulting in sustained activation of Bax (Fig. 6 *D*). This is consistent with the experimental observation that p53 can induce apoptosis in PUMA-deficient Bcl-$xL^{-/-}$ cells (13). Therefore, our results verify that liberation of cytoplasmic p53 from Bcl-xL is a critical event in the direct activation of Bax by p53. Our results also suggest that PFT-μ may be able to reactivate the proapoptotic function of cytoplasmic p53 in PUMA-deficient tumor cells.

Effect of p53 localization on cell fate decision

We have revealed the role of PUMA in coupling the nuclear and cytoplasmic functions of p53. Here, we further investigate the effect of subcellular distribution of p53 on cell fate decision by changing its nuclear export rate k_{p53n}. We calculate the maximal protein levels on each simulation trial; they exhibit different dependence on k_{p53n} (Fig. 7 *A*). Clearly, $[p53_c^*]_{max}$ rises with increasing k_{p53n} when $k_{p53n} \leq 3.1\ min^{-1}$, whereas $[p53_n]_{max}$ and $[PUMA^*]_{max}$ decrease monotonically. Differently, $[Bax^*]_{max}$ exhibits a nonmonotonic behavior. $[PUMA]_T$ and $[Bax]_T$ are mainly determined by $[p53_n]$, while [Bax*] remarkably depends on $[p53_c^*]$ and $[Bax]_T$. Lack of nuclear p53 greatly reduces the expression of Bax, while lack of free cytoplasmic p53 suppresses the activation of Bax. Thus, [Bax*] depends on both the nuclear and cytoplasmic levels of p53; $[Bax^*]_{max}$ reaches a maximum at $k_{p53n} \sim 1.28$. When $k_{p53n} > 3.1$, the amount of free cytoplasmic p53 decreases with increasing k_{p53n} because of very low PUMA* level, and $[Bax^*]_{max}$ is smaller than the threshold for apoptosis induction. That is, excessive nuclear export of p53 makes cells resistant to lethal DNA damage. This is consistent with the experimental observations in neuroblastoma cells, where remarkable exclusion of p53 from the nucleus leads to deficiency in apoptosis induction (37,38). Similarly, when $k_{p53n} < 0.16$, $[Bax^*]_{max}$ is also smaller than the threshold for apoptosis induction. Thus, a balance between the nuclear and cytoplasmic p53 levels is crucial for the full activation of apoptosis.

For each k_{p53n}, there exists a minimal extent of DNA damage for apoptosis induction, DNA_{dam}^c, which takes a minimum at $k_{p53n} \sim 0.2\ min^{-1}$ (Fig. 7 *B*). For $k_{p53n} < 0.13$, a small amount of cytoplasmic p53 is insufficient to activate Bax to induce apoptosis when $DNA_{dam}^0 < 10$. Similarly, for $k_{p53n} > 3.2$, a low level of nuclear p53 is unable to induce enough PUMA and Bax, and no apoptosis is triggered when $DNA_{dam}^0 < 10$. In the above cases, cells become resistant to apoptosis. By contrast, for $0.16 \leq k_{p53n} \leq 0.68$, apoptosis can be induced in response to DNA damage with $DNA_{dam}^0 > 5$. Together, we conclude that excessive accumulation of p53 in either compartment makes cells resistant to apoptotic signals, and both the nuclear and cytoplasmic activities of p53 are indispensable for reliable cell fate decision. This awaits experimental validation.

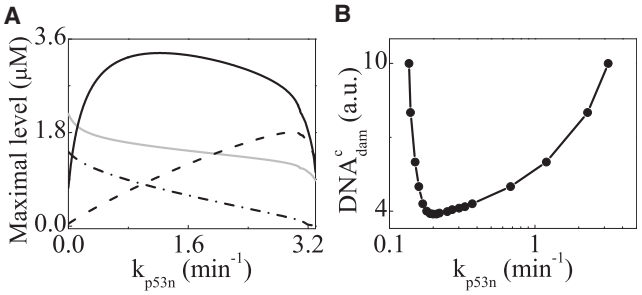

FIGURE 7 Effect of subcellular localization of p53 on cell fate decision. (*A*) The maximal levels of $p53_n$ (*shaded line*), $p53_c^*$ (*dashed line*), PUMA* (*dash-dotted line*), and Bax* (*solid line*) versus the nuclear export rate of p53, k_{p53n}. The initial stress level is 6.0. (*B*) The minimal extent of DNA damage for apoptosis induction, DNA_{dam}^c, versus k_{p53n}.

Akt acting as a gatekeeper for apoptosis induction

While coordination of the nuclear and cytoplasmic activities of p53 is vital to cell fate decision, cross-talk between p53 and Akt also mediates cellular responses. As mentioned above, p53 and Akt antagonize each other through a double-negative feedback. Specifically, Akt can counteract the effect of p53 on apoptosis induction by promoting the nuclear translocation of Mdm2. By contrast, p53-inducible PTEN can suppress Akt activity to enhance the proapoptotic function of p53.

Fig. 8 *A* shows the steady-state bifurcation diagram of $p53_n$ and Akt_p levels versus DNA_{dam}. They share the same bistability range but exhibit totally opposite switching behaviors. In fact, when Akt_p level is in the upper branch, $p53_n$ level is in the lower branch, and vice versa. This is because either p53 or Akt achieves self-accumulation by inhibiting the other. Indeed, the increase in DNA_{dam} promotes $p53_n$ accumulation, and the subsequent deactivation of Akt further enhances the accumulation of $p53_n$.

The effect of Akt on cell fate decision is explored by varying the total Akt level. We first study the bifurcation diagrams of Bax* level versus DNA_{dam} for various $[Akt]_T$ (Fig. 8 *B*). For small $[Akt]_T$ (e.g., 0.15 μM), the threshold

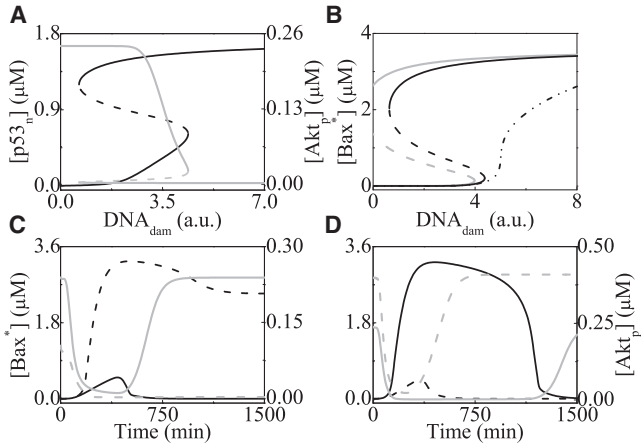

FIGURE 8 Effect of Akt on cell fate decision. (*A*) Steady-state bifurcation diagram of $p53_n$ (*black line*) and Akt_p (*shaded line*) levels versus the extent of DNA damage with $[Akt]_T = 0.5\ \mu M$. (*B*) Bifurcation diagram of Bax* level with $[Akt]_T = 0.15$ (*shaded line*), 0.5 (*black line*), or 5 μM (*dash-dot-dotted line*). (*C* and *D*) Time courses of Bax* (*black lines*) and Akt_p (*shaded lines*) levels with $[Akt]_T = 0.15$ (*dashed lines*) or 0.5 μM (*solid lines*) at $DNA_{dam}^0 = 5.2$ (*C*); with $[Akt]_T = 0.5$ (*solid lines*) or 5 μM (*dashed lines*) at $DNA_{dam}^0 = 6.0$ (*D*).

value of DNA_{dam} for Bax activation is relatively small, and the switching is irreversible. Once Bax is activated, it remains active. The threshold value gets smaller with further decreasing $[Akt]_T$, and cells become more sensitive to DNA damage, so that even mild damage can induce apoptosis. When $[Akt]_T$ is within the range of 0.18~4.8 μM, Bax* level exhibits reversible bistability, and the bistability range shrinks with increasing $[Akt]_T$. For large $[Akt]_T$ (say 5.0 μM), Bax* level exhibits monostability and varies sigmoidally with DNA_{dam}. Only when DNA_{dam} is large enough can Bax* level be kept at large values. In sum, Bax* levels exhibit irreversible and reversible bistability and monostability, respectively, with increasing $[Akt]_T$.

Next, we show the temporal evolution of Akt_p and Bax* levels for various $[Akt]_T$ values at distinct stress intensity. In unstressed cells, most Akt molecules are phosphorylated and activated, whereas levels of the proapoptotic proteins are kept low. Upon DNA damage, $p53_n$ accumulates and PTEN is expressed, whereas Akt phosphorylation is reversed. If DNA damage is repairable, Bax* abundance drops to basal levels and Akt is rephosphorylated after transients (Fig. 8 *C*). With $[Akt]_T$ reduced, however, even mild DNA damage can induce apoptosis. That is, lack of Akt makes cells rather sensitive to DNA damage, and accidental stress may threaten cell survival. For example, only a small amount of Akt has been detected in brain samples from Huntington patients, leading to neuronal dysfunction and death (39). In the case of severe DNA damage, a high Bax* level is maintained, whereas most Akt molecules are dephosphorylated (Fig. 8 *D*). Consequently, apoptosis is induced. With increased $[Akt]_T$, however, even severely damaged cells may escape from apoptosis. Thus, cells become resistant to DNA damage, which greatly increases the risk of tumorigenesis. Our results are consistent with the role of Akt as an oncoprotein (15). Together, Akt levels should be controlled to guarantee the balance between cell survival and death.

SUMMARY AND DISCUSSION

We have characterized coordination between the nuclear and cytoplasmic p53 pathways in response to DNA damage. In our model, both the negative feedback loop between p53 and Mdm2 and the positive one involving p53, Akt and Mdm2 are considered. Consequently, the switching between low and high protein levels underlies the decision between cell survival and death. Upon DNA damage, destabilization of Mdm2 leads to accumulation of p53 in the nucleus and cytoplasm, as well as deactivation of Akt by dephosphorylation. Nuclear p53 induces expression of *Mdm2*, *PTEN*, *PUMA*, and *Bax*. Subsequently, cytoplasmic p53 is released from Bcl-xL by PUMA to activate Bax directly; sustained activation of Bax induces apoptosis. Depending on the initial stress intensity, cells either survive or die. Both the nuclear and cytoplasmic functions of p53 are important for cell fate decision; deficiency of p53 in either compartment makes stressed cells resistant to death signals. Moreover, Akt can suppress p53 activity, and its appropriate levels contribute to the balance between cell survival and death.

p53 is primarily a nuclear protein, acting as a transcription factor (4). Cytoplasmic sequestration of p53 may interfere with its transcriptional function (40). Indeed, excessive accumulation of cytoplasmic p53 appears to promote inactivation of p53 in tumors (37,38). However, cytoplasmic p53 can also activate Bax directly through a transcription-independent mechanism (11,12), and PUMA can couple the nuclear and cytoplasmic functions of p53 in response to genotoxic stress (13). Here, we further demonstrate that such coordinated p53 activities contribute to cell fate decision; thus, the limitation associated with individual p53 pathways may be overcome. For example, it was reported that the transcription-independent p53 pathway is activated to induce apoptosis rather than cell cycle arrest (41) and that the transcription-dependent pathway can only initiate cell cycle arrest in some tissues (42). By contrast, coordination of the transcription-dependent and -independent functions of p53 subserves making reliable decisions by integrating diverse signals.

Cytoplasmic p53 behaves as an activator, like the BH3-only proteins Bid and Bim, activating Bax directly, whereas mitochondrial p53 can act as an enabler to activate Bax indirectly by releasing Bax from its inhibitor (11). The binding of cytoplasmic p53 to Bcl-xL is antiapoptotic (13), whereas that of mitochondrial p53 to Bcl-xL is proapoptotic (43). Moreover, it has recently been reported that the small molecule PFT-μ can inhibit the proapoptotic activity of mitochondrial p53 by reducing its affinity for Bcl-xL (36), whereas our results suggest that PFT-μ may enhance the proapoptotic function of cytoplasmic p53. Thus, with PFT-μ as a probe, the role of p53 in apoptosis induction can be distinguished between an enabler and an activator, which may allow for pertinent treatment of some cancers. It would also be intriguing to explore the possible coordination among nuclear, cytoplasmic, and mitochondrial p53 pathways in response to stresses.

Our results are in good agreement with experimental observations. Chipuk et al. (13) have demonstrated in mutation experiments on Bcl-xL that the release of cytoplasmic p53 from Bcl-xL by PUMA is required to induce apoptosis. In our simulations, decreasing the binding affinity of PUMA to Bcl-xL does make cells more resistant to DNA damage. Furthermore, decreasing the synthesis rate of PUMA has a similar effect. Thus, modulating the proapoptotic activity of PUMA is an efficient way to regulate apoptosis development. Actually, deletion of *PUMA* abrogates p53-induced apoptosis and greatly increases the risk of tumorigenesis (34,35). Given the potential role of some small-molecule inhibitors, like PFT-μ, in liberating cytoplasmic p53 from its inhibitor, a possible strategy for tumor therapy is to utilize them to reactivate or potentiate the proapoptotic function of cytoplasmic p53.

The p53 dynamics are actually cell-, tissue-, and stress-dependent in the DNA damage response (4). To our knowledge, oscillatory p53 dynamics in response to UV radiation were suggested only in one experiment (44), with a period (15 ~20 h) much longer than the typical one (5 ~7 h) in cellular responses to ionizing radiation (18,45). No evidence suggests the existence of p53 oscillations in the experiment by Chipuk et al. (13). Nevertheless, it is still worth experimentally exploring whether p53 oscillations exist in the UV response of other cells. Undoubtedly, the negative feedback between p53 and Mdm2 is the basis of p53 oscillations. However, it was proposed that the positive feedback loop involving p53, PTEN, Akt, and Mdm2 can terminate oscillations induced by the p53-Mdm2 loop and enable p53 abundance to rise to high levels (46). In our model, p53 and PTEN are activated almost simultaneously. Thus, the positive feedback loop becomes dominant over the negative one, and p53 levels show a switchlike behavior.

Akt levels should be controlled within a proper range. Either deficiency or excessive expression of Akt may destroy the balance between cell life and death, leading to improper cellular outcomes. Overexpression of Akt has been observed in several cancer cell lines (15), whereas lack of Akt makes cells ultrasensitive to stress signals and leads to diseases in animals and humans (39). Moreover, for the sake of simplicity, only the role of Akt in suppressing accumulation of nuclear p53 is considered in our model. In fact, Akt can also inhibit apoptosis through repressing the activities of other proapoptotic factors such as Bad and several caspases (47). Thus, a more detailed model may be helpful to thoroughly explore the effect of Akt on cell fate decision.

It is worth noting that a couple of aspects of p53 regulation are not considered in our model. First, here we include only two feedback loops involving p53. The p53-Mdm2 negative feedback loop is the core of p53 regulation (48), and the p53-Akt-Mdm2 positive feedback loop is significant for the p53-mediated decision between cell life and death (22). Nevertheless, there also exists another negative feedback loop between p53 and Wip1, in which p53-induced Wip1 decreases the level and activity of p53 by dephosphorylating p53, Mdm2, ATM, and Chk1 (49). This loop may act as a gatekeeper for the p53-Mdm2 loop and set a barrier for p53 activation and apoptosis induction. Presumably, adding this loop to our model would increase the threshold for apoptosis induction, but not qualitatively change our main conclusions. Second, we did not explicitly consider posttranslational modifications of p53, which may have an important role in cell fate decision (4). For example, the phosphorylation of p53 at Serine 46 promotes expression of the proapoptotic gene *p53AIP1* (50). Moreover, some posttranslational modifications of p53 can affect its subcellular localization (4). Thus, an extended model should be constructed to explore these effects in the future.

In this work we explored the mechanism for cell fate decision after DNA damage based on the nuclear and cytoplasmic p53 pathways. Our study points to the central roles of p53, PUMA, and Akt. First, p53 is stabilized and accumulates in both the nucleus and cytoplasm upon DNA damage, and then induces different cellular outcomes including survival and apoptosis. Second, PUMA acts as a coordinator coupling the nuclear and cytoplasmic activities of p53. Dysfunction of PUMA may greatly increase the risk of tumorigenesis or lead to unnecessary death of repairable cells. Third, Akt can modulate cellular responses, acting as a gatekeeper for p53-dependent apoptosis. An appropriate Akt level is vital to reliable cell fate decision. These results enrich the understanding of how the p53 network responds to various stresses and may provide clues to p53-based cancer therapy.

APPENDIX

The dynamic equations of the model are presented as follows:

$$\frac{d\mathrm{DNA_{dam}}}{dt} = -k_{\mathrm{rep}}\theta(\mathrm{DNA_{dam}}) \tag{1}$$

$$\begin{aligned}\frac{d[\mathrm{p53_n}]}{dt} = {} & -k_{\mathrm{p53n}}[\mathrm{p53_n}] + k_{\mathrm{p53c}}\left[\mathrm{p53_c^*}\right] \\ & - k_{\mathrm{dmp53n}}[\mathrm{Mdm2_n}]\frac{[\mathrm{p53_n}]}{[\mathrm{p53_n}] + J_{\mathrm{dmp53n}}} \\ & - k_{\mathrm{dp53n}}[\mathrm{p53_n}]\end{aligned} \tag{2}$$

$$\begin{aligned}\frac{d[\mathrm{p53 \cdot Bcl\text{-}xL}]}{dt} = {} & k_{\mathrm{p53i}}\left[\mathrm{p53_c^*}\right][\mathrm{Bcl\text{-}xL}] \\ & - k_{\mathrm{p53a}}[\mathrm{PUMA^*}][\mathrm{p53 \cdot Bcl\text{-}xL}] \\ & - k_{\mathrm{p53a0}}[\mathrm{p53 \cdot Bcl\text{-}xL}] \\ & - k_{\mathrm{dp53bx}}[\mathrm{p53 \cdot Bcl\text{-}xL}]\end{aligned} \tag{3}$$

$$\begin{aligned}\frac{d\left[\mathrm{p53_c^*}\right]}{dt} = {} & k_{\mathrm{p53}} + k_{\mathrm{p53n}}[\mathrm{p53_n}] - k_{\mathrm{p53c}}\left[\mathrm{p53_c^*}\right] \\ & + k_{\mathrm{p53a}}[\mathrm{PUMA^*}][\mathrm{p53 \cdot Bcl\text{-}xL}] \\ & + k_{\mathrm{p53a0}}[\mathrm{p53 \cdot Bcl\text{-}xL}] \\ & - k_{\mathrm{p53i}}\left[\mathrm{p53_c^*}\right][\mathrm{Bcl\text{-}xL}] - k_{\mathrm{dp53cs}}\left[\mathrm{p53_c^*}\right] \\ & - k_{\mathrm{dmp53cs}}[\mathrm{Mdm2_c}]\frac{\left[\mathrm{p53_c^*}\right]}{\left[\mathrm{p53_c^*}\right] + J_{\mathrm{dmp53cs}}}\end{aligned} \tag{4}$$

$$\begin{aligned}\frac{d[\mathrm{Mdm2_n}]}{dt} = {} & -k_{\mathrm{m2n}}[\mathrm{Mdm2_n}] + k_{\mathrm{m2c}}\left[\mathrm{Mdm2_{cp}}\right] \\ & - k_{\mathrm{dm2n}}[\mathrm{Mdm2_n}] - k_{\mathrm{dm2n0}} \times \mathrm{DNA_{dam}} \\ & \times [\mathrm{Mdm2_n}]\end{aligned} \tag{5}$$

$$\frac{d[\mathrm{Mdm2_c}]}{dt} = k_{\mathrm{m2}} + k'_{\mathrm{m2}}\frac{[\mathrm{p53_n}]^4}{[\mathrm{p53_n}]^4 + J_1^4} + k_{\mathrm{m2dp}}\frac{[\mathrm{Mdm2_{cp}}]}{[\mathrm{Mdm2_{cp}}] + J_{\mathrm{m2dp}}} - k_{\mathrm{m2p}}[\mathrm{Akt_p}]\frac{[\mathrm{Mdm2_c}]}{[\mathrm{Mdm2_c}] + J_{\mathrm{m2p}}} - k_{\mathrm{dm2c}}[\mathrm{Mdm2_c}] \quad (6)$$

$$\frac{d[\mathrm{Mdm2_{cp}}]}{dt} = k_{\mathrm{m2n}}[\mathrm{Mdm2_n}] - k_{\mathrm{m2c}}[\mathrm{Mdm2_{cp}}] + k_{\mathrm{m2p}}[\mathrm{Akt_p}]\frac{[\mathrm{Mdm2_c}]}{[\mathrm{Mdm2_c}] + J_{\mathrm{m2p}}} - k_{\mathrm{m2dp}}\frac{[\mathrm{Mdm2_{cp}}]}{[\mathrm{Mdm2_{cp}}] + J_{\mathrm{m2dp}}} - k_{\mathrm{dm2cp}}[\mathrm{Mdm2_{cp}}] \quad (7)$$

$$\frac{d[\mathrm{Akt_p}]}{dt} = k_{\mathrm{aktp}}[\mathrm{PIP3}]\frac{[\mathrm{Akt}]}{[\mathrm{Akt}] + J_{\mathrm{aktp}}} - k_{\mathrm{aktdp}}\frac{[\mathrm{Akt_p}]}{[\mathrm{Akt_p}] + J_{\mathrm{aktdp}}} \quad (8)$$

$$\frac{d[\mathrm{PIP3}]}{dt} = k_{\mathrm{PIP3}}\frac{[\mathrm{PIP2}]}{[\mathrm{PIP2}] + J_{\mathrm{PIP3}}} - k_{\mathrm{PIP2}}[\mathrm{PTEN}]\frac{[\mathrm{PIP3}]}{[\mathrm{PIP3}] + J_{\mathrm{PIP2}}} \quad (9)$$

$$\frac{d[\mathrm{PTEN}]}{dt} = k_{\mathrm{PTEN}} + k'_{\mathrm{PTEN}}\frac{[\mathrm{p53_n}]^4}{[\mathrm{p53_n}]^4 + J_2^4} - k_{\mathrm{dPTEN}}[\mathrm{PTEN}] \quad (10)$$

$$\frac{d[\mathrm{Bcl\text{-}xL}]_{\mathrm{T}}}{dt} = k_{\mathrm{B}} - k_{\mathrm{dB}}[\mathrm{Bcl\text{-}xL}]_{\mathrm{T}} \quad (11)$$

$$\frac{d[\mathrm{PUMA}]_{\mathrm{T}}}{dt} = k_{\mathrm{puma}} + k'_{\mathrm{puma}}\frac{[\mathrm{p53_n}]^4}{[\mathrm{p53_n}]^4 + J_3^4} - k_{\mathrm{dpuma}}[\mathrm{PUMA}]_{\mathrm{T}} \quad (12)$$

$$\frac{d[\mathrm{PUMA \cdot Bcl\text{-}xL}]}{dt} = k_{\mathrm{p53a}}[\mathrm{PUMA^*}][\mathrm{p53 \cdot Bcl\text{-}xL}] + k_{\mathrm{pumai}}[\mathrm{PUMA^*}][\mathrm{Bcl\text{-}xL}] - k_{\mathrm{pumaa0}}[\mathrm{PUMA \cdot Bcl\text{-}xL}] \quad (13)$$

$$\frac{d[\mathrm{Bax}]_{\mathrm{T}}}{dt} = k_{\mathrm{bax}} + k'_{\mathrm{bax}}\frac{[\mathrm{p53_n}]^4}{[\mathrm{p53_n}]^4 + J_4^4} - k_{\mathrm{dbax}}[\mathrm{Bax}]_{\mathrm{T}} \quad (14)$$

$$\frac{d[\mathrm{Bax^*}]}{dt} = k_{\mathrm{baxa}}[\mathrm{p53_c^*}][\mathrm{Bax_{in}}] - k_{\mathrm{baxi}}[\mathrm{Bax^*}] \quad (15)$$

$$[\mathrm{Akt}]_{\mathrm{T}} = [\mathrm{Akt_p}] + [\mathrm{Akt}] \quad (16)$$

$$[\mathrm{PIP}]_{\mathrm{T}} = [\mathrm{PIP3}] + [\mathrm{PIP2}] \quad (17)$$

$$[\mathrm{Bcl\text{-}xL}]_{\mathrm{T}} = [\mathrm{Bcl\text{-}xL}] + [\mathrm{p53 \cdot Bcl\text{-}xL}] + [\mathrm{PUMA \cdot Bcl\text{-}xL}] \quad (18)$$

$$[\mathrm{PUMA}]_{\mathrm{T}} = [\mathrm{PUMA^*}] + [\mathrm{PUMA \cdot Bcl\text{-}xL}] \quad (19)$$

$$[\mathrm{Bax}]_{\mathrm{T}} = [\mathrm{Bax^*}] + [\mathrm{Bax_{in}}] \quad (20)$$

$$\theta(x) = \begin{cases} 1 & x \geq 0 \\ 0 & x < 0 \end{cases} \quad (21)$$

This work was supported by the National Natural Science Foundation of China (grant No. 10604028), the National Basic Research Program of China (grant No. 2007CB814806), the Natural Science Foundation of Jiangsu Province (grant No. SBK200910089), the Program for New Century Excellent Talents in University (grant No. 08-0269), and the Scientific Research Foundation for the Returned Overseas Chinese Scholars.

REFERENCES

1. Vogelstein, B., D. Lane, and A. J. Levine. 2000. Surfing the p53 network. *Nature.* 408:307–310.
2. Vousden, K. H., and D. P. Lane. 2007. p53 in health and disease. *Nat. Rev. Mol. Cell Biol.* 8:275–283.
3. Haupt, Y., R. Maya, …, M. Oren. 1997. Mdm2 promotes the rapid degradation of p53. *Nature.* 387:296–299.
4. Murray-Zmijewski, F., E. A. Slee, and X. Lu. 2008. A complex barcode underlies the heterogeneous response of p53 to stress. *Nat. Rev. Mol. Cell Biol.* 9:702–712.
5. Vousden, K. H. 2006. Outcomes of p53 activation—spoilt for choice. *J. Cell Sci.* 119:5015–5020.
6. Wang, P., J. Yu, and L. Zhang. 2007. The nuclear function of p53 is required for PUMA-mediated apoptosis induced by DNA damage. *Proc. Natl. Acad. Sci. USA.* 104:4054–4059.
7. Nakano, K., and K. H. Vousden. 2001. PUMA, a novel proapoptotic gene, is induced by p53. *Mol. Cell.* 7:683–694.
8. Miyashita, T., and J. C. Reed. 1995. Tumor suppressor p53 is a direct transcriptional activator of the human Bax gene. *Cell.* 80:293–299.
9. Green, D. R., and G. Kroemer. 2009. Cytoplasmic functions of the tumor suppressor p53. *Nature.* 458:1127–1130.
10. Moll, U. M., S. Wolff, …, W. Deppert. 2005. Transcription-independent pro-apoptotic functions of p53. *Curr. Opin. Cell Biol.* 17:631–636.
11. Speidel, D. 2010. Transcription-independent p53 apoptosis: an alternative route to death. *Trends Cell Biol.* 20:14–24.
12. Chipuk, J. E., T. Kuwana, …, D. R. Green. 2004. Direct activation of Bax by p53 mediates mitochondrial membrane permeabilization and apoptosis. *Science.* 303:1010–1014.
13. Chipuk, J. E., L. Bouchier-Hayes, …, D. R. Green. 2005. PUMA couples the nuclear and cytoplasmic proapoptotic function of p53. *Science.* 309:1732–1735.
14. Cory, S., and J. M. Adams. 2002. The Bcl2 family: regulators of the cellular life-or-death switch. *Nat. Rev. Cancer.* 2:647–656.

15. Vivanco, I., and C. L. Sawyers. 2002. The phosphatidylinositol 3-kinase-Akt pathway in human cancer. *Nat. Rev. Cancer.* 2:489–501.

16. Datta, S. R., H. Dudek, …, M. E. Greenberg. 1997. Akt phosphorylation of BAD couples survival signals to the cell-intrinsic death machinery. *Cell.* 91:231–241.

17. Gottlieb, T. M., J. F. M. Leal, …, M. Oren. 2002. Cross-talk between Akt, p53 and Mdm2: possible implications for the regulation of apoptosis. *Oncogene.* 21:1299–1303.

18. Lahav, G., N. Rosenfeld, …, U. Alon. 2004. Dynamics of the p53-Mdm2 feedback loop in individual cells. *Nat. Genet.* 36:147–150.

19. Zhang, X.-P., F. Liu, …, W. Wang. 2009. Cell fate decision mediated by p53 pulses. *Proc. Natl. Acad. Sci. USA.* 106:12245–12250.

20. Zhang, T., P. Brazhnik, and J. J. Tyson. 2007. Exploring mechanisms of the DNA-damage response: p53 pulses and their possible relevance to apoptosis. *Cell Cycle.* 6:85–94.

21. Sun, T., C. Chen, …, P. Shen. 2009. Modeling the role of p53 pulses in DNA damage- induced cell death decision. *BMC Bioinformatics.* 10:190.

22. Wee, K. B., and B. D. Aguda. 2006. Akt versus p53 in a network of oncogenes and tumor suppressor genes regulating cell survival and death. *Biophys. J.* 91:857–865.

23. Mayo, L. D., and D. B. Donner. 2001. A phosphatidylinositol 3-kinase/Akt pathway promotes translocation of Mdm2 from the cytoplasm to the nucleus. *Proc. Natl. Acad. Sci. USA.* 98:11598–11603.

24. Stambolic, V., D. MacPherson, …, T. W. Mak. 2001. Regulation of PTEN transcription by p53. *Mol. Cell.* 8:317–325.

25. Cantley, L. C., and B. G. Neel. 1999. New insights into tumor suppression: PTEN suppresses tumor formation by restraining the phosphoinositide 3-kinase/AKT pathway. *Proc. Natl. Acad. Sci. USA.* 96: 4240–4245.

26. Boehme, K. A., R. Kulikov, and C. Blattner. 2008. p53 stabilization in response to DNA damage requires Akt/PKB and DNA-PK. *Proc. Natl. Acad. Sci. USA.* 105:7785–7790.

27. Chipuk, J. E., and D. R. Green. 2008. How do BCL-2 proteins induce mitochondrial outer membrane permeabilization? *Trends Cell Biol.* 18:157–164.

28. Ma, L., J. Wagner, …, G. A. Stolovitzky. 2005. A plausible model for the digital response of p53 to DNA damage. *Proc. Natl. Acad. Sci. USA.* 102:14266–14271.

29. Jiang, Y., C. Ke, …, P. E. Marszalek. 2007. Detecting ultraviolet damage in single DNA molecules by atomic force microscopy. *Biophys. J.* 93:1758–1767.

30. Goldstein, J. C., N. J. Waterhouse, …, D. R. Green. 2000. The coordinate release of cytochrome *c* during apoptosis is rapid, complete and kinetically invariant. *Nat. Cell Biol.* 2:156–162.

31. Pagliari, L. J., T. Kuwana, …, D. R. Green. 2005. The multidomain proapoptotic molecules Bax and Bak are directly activated by heat. *Proc. Natl. Acad. Sci. USA.* 102:17975–17980.

32. Earnshaw, W. C., L. M. Martins, and S. H. Kaufmann. 1999. Mammalian caspases: structure, activation, substrates, and functions during apoptosis. *Annu. Rev. Biochem.* 68:383–424.

33. Chen, C., J. Cui, …, P. Shen. 2007. Modeling of the role of a Bax-activation switch in the mitochondrial apoptosis decision. *Biophys. J.* 92:4304–4315.

34. Yu, J., Z. Wang, …, L. Zhang. 2003. PUMA mediates the apoptotic response to p53 in colorectal cancer cells. *Proc. Natl. Acad. Sci. USA.* 100:1931–1936.

35. Karst, A. M., D. L. Dai, …, G. Li. 2005. PUMA expression is significantly reduced in human cutaneous melanomas. *Oncogene.* 24: 1111–1116.

36. Strom, E., S. Sathe, …, A. V. Gudkov. 2006. Small-molecule inhibitor of p53 binding to mitochondria protects mice from gamma radiation. *Nat. Chem. Biol.* 2:474–479.

37. Sengupta, S., J.-L. Vonesch, …, B. Wasylyk. 2000. Negative cross-talk between p53 and the glucocorticoid receptor and its role in neuroblastoma cells. *EMBO J.* 19:6051–6064.

38. Lu, W., R. Pochampally, …, J. Chen. 2000. Nuclear exclusion of p53 in a subset of tumors requires MDM2 function. *Oncogene.* 19:232–240.

39. Colin, E., E. Régulier, …, F. Saudou. 2005. Akt is altered in an animal model of Huntington's disease and in patients. *Eur. J. Neurosci.* 21:1478–1488.

40. O'Brate, A., and P. Giannakakou. 2003. The importance of p53 location: nuclear or cytoplasmic zip code? *Drug Resist. Updat.* 6:313–322.

41. Marchenko, N. D., A. Zaika, and U. M. Moll. 2000. Death signal-induced localization of p53 protein to mitochondria. A potential role in apoptotic signaling. *J. Biol. Chem.* 275:16202–16212.

42. Fei, P., E. J. Bernhard, and W. S. El-Deiry. 2002. Tissue-specific induction of p53 targets in vivo. *Cancer Res.* 62:7316–7327.

43. Mihara, M., S. Erster, …, U. M. Moll. 2003. p53 has a direct apoptogenic role at the mitochondria. *Mol. Cell.* 11:577–590.

44. Collister, M., D. P. Lane, and B. L. Kuehl. 1998. Differential expression of p53, p21waf1/cip1 and hdm2 dependent on DNA damage in Bloom's syndrome fibroblasts. *Carcinogenesis.* 19:2115–2120.

45. Ramalingam, S., P. Honkanen, …, S. Nishizuka. 2007. Quantitative assessment of the p53-Mdm2 feedback loop using protein lysate microarrays. *Cancer Res.* 67:6247–6252.

46. Puszyński, K., B. Hat, and T. Lipniacki. 2008. Oscillations and bistability in the stochastic model of p53 regulation. *J. Theor. Biol.* 254: 452–465.

47. Manning, B. D., and L. C. Cantley. 2007. AKT/PKB signaling: navigating downstream. *Cell.* 129:1261–1274.

48. Harris, S. L., and A. J. Levine. 2005. The p53 pathway: positive and negative feedback loops. *Oncogene.* 24:2899–2908.

49. Lu, X., O. Ma, …, L. A. Donehower. 2007. The Wip1 Phosphatase acts as a gatekeeper in the p53-Mdm2 autoregulatory loop. *Cancer Cell.* 12:342–354.

50. Oda, K., H. Arakawa, …, Y. Taya. 2000. p53AIP1, a potential mediator of p53-dependent apoptosis, and its regulation by Ser-46-phosphorylated p53. *Cell.* 102:849–862.